JOURNAL OF BIOMEDICAL OPTICS 4(2), 200–207 (APRIL 1999)

# PANORAMIC OPTICAL IMAGING OF ELECTRICAL PROPAGATION IN ISOLATED HEART

**Shien-Fong Lin and John P. Wikswo, Jr.**
Vanderbilt University, Department of Physics and Astronomy, Nashville, Tennessee 37235
(Paper JBO-170 received Sep. 12, 1997; revised manuscript received Oct. 30, 1998; accepted for publication Jan. 6, 1999.)

## ABSTRACT

Optical imaging of cardiac transmembrane potential in dye-stained tissue is an emerging technique in cardiac electrophysiology. Despite its widespread application to studies of isolated hearts, it has been applied traditionally to recording only a single view that presents the potential distribution of a fraction of the cardiac surface. This poses a significant limitation in studying whole heart electrophysiology, particularly when large-scale phenomena such as fibrillation and defibrillation are of interest. We have developed a panoramic imaging system based on a high-speed charge-coupled device camera with a maximum imaging speed of 335 frames/s at 128×64 pixels/frame. Our system provides one front view and two back mirror views of isolated hearts, thus extending optical imaging capabilities to record from the entire three dimensional heart surface with only one camera. © *1999 Society of Photo-Optical Instrumentation Engineers.* [S1083-3668(99)00102-1]

**Keywords** heart; fluorescence; laser; optical fiber; bioinstrument.

## 1 INTRODUCTION

One of the major objectives in cardiac electrophysiology is to characterize the distribution of transmembrane potential ($V_m$) at all points of the myocardium during normal propagation, as well as during fibrillation and defibrillation. In the most commonly used approach, an electrode array is used to map the epicardial potentials, with the evolution of the technique leading to a steady increase in the number and the density of electrodes, limited by electrode size, array complexity, and data acquisition system cost; seldom are more than 500 data acquisition channels available. Moreover, in most cases, the electrodes and the connection wires are cumbersome to install and difficult to reconfigure, and electrode location must be determined for each experiment. On the other hand, an emerging technique in cardiac mapping is to record optically the transmembrane potential using potentiometric dyes. Developed around the principle of staining the tissue with voltage-sensitive dyes and recording the variation in the intensity of the induced epifluorescence, such techniques provide an indirect estimate of the transmembrane potentials. A variety of approaches based on different light-sensing components, including photodiode arrays, photomultiplier tubes, and charge-coupled device (CCD) cameras, have been utilized to measure the transmembrane potential distribution during different electrical states in cardiac tissue.[1–5] Different illumination sources such as argon lasers, halogen lamps, and solid-state lasers have been used in conjunction with the light collecting devices.

One of the most important system characteristics in designing a cardiac optical recording system is the trade-off between the temporal and spatial resolutions. For example, photodiode arrays offer a temporal resolution of greater than 1000 Hz per recording site, but the number of recording sites is typically limited to less than 300.[6,7] On the other hand, a large format CCD camera offers high spatial resolution of approximately 250 000 pixels, but its temporal resolution has been limited to 60 fields/s.[1] Recently, with improving CCD technology and increased data transfer rates, this spatial-temporal resolution trade-off is becoming a less restrictive factor. An additional consideration in optical mapping is the ''field of view,'' which was previously limited to imaging only a single view of a fraction of the cardiac surface. Traditionally, imaging is a two dimensional (2D) process that maps a three dimensional (3D) object to a single 2D CCD or photodiode array sensor. An approach for imaging a three dimensional heart is to use multiple CCD cameras to obtain more than one view of cardiac propagation, but this approach is expensive in that it requires not only multiple high-speed cameras, but also a frame grabber for each camera and requires synchronization of the cameras. However, some newer frame grabbers employ a 32 bit data

Address correspondence to Shien-Fong Lin, Department of Physics and Astronomy, Vanderbilt University, P.O. Box 1807, Station B, Nashville, TN 37235. Electronic mail: linsf@ctrvax.vanderbilt.edu

width, thus allow multiple taps image acquisition with only one frame grabber board. The panoramic imaging technique developed in this study is to use mirrors to image the entire heart surface with a single high-speed digital camera, providing the capability to image asynchronous events such as arrhythmias and fibrillation from the whole heart. We adopted the one-camera approach in order to facilitate the experimental setup. It should be noted that ''panorama'' usually refers to an observer-centered full view of the surrounding environment. In this paper, we use panorama to represent an object-centered complete view of the heart.

## 2 MATERIALS AND METHODS

### 2.1 IMAGING SYSTEM

The optical sensing device of the imaging system is a digital CCD camera with 12 bit data digitization (model CA-D1-0256T, Dalsa Inc., Waterloo, ON, Canada), with a 25 mm/$f$0.85 video lens (CF25L, Fujinon) attached to the lens mount port. The CCD camera has 256×256 photoelements with a pixel size of 16×16 $\mu$m$^2$. The camera can operate in a 2×2 binning mode to speed up the acquisition and to increase light collecting efficiency, providing a 128×128 square image format. To register all three views of the heart, a 128×64 pixel region of interest was acquired and stored. The faceplate of the camera was cooled with an ethylene-glycol coolant from a refrigerated water bath to 15°C from a normal operating temperature of greater than 30°C. The cooling of the camera reduced the dark current by fourfold to a digitized output of less than 100, i.e., about 2.5% of the 4096 digitized levels with 12 bit analog-to-digital conversion.

The data from the digital camera were transferred to a PCI bus-master frame grabber board (IC-PCI, Imaging Technology Inc., Bedford, MA) mounted in an IBM-compatible personal computer (Millennia Pro2 Plus, Micron Computer). Image acquisition was controlled by Eye Image Calculator (IO Industries Inc., London, ON, Canada) modified to include external trigger capability. The imaging system has a maximal frame rate of 335 frames/s, with a frame interval of 2.98 ms. When taking a time sequence of images, the number of frames that can be acquired is limited by the amount of computer on-board random-access memory (RAM). However, in order to limit the storage and analysis requirements, an acquired sequence typically consists of 300–600 frames, representing a total recording time of approximately 1–2 s, and requiring 4800–9600 Kbytes of RAM. It is possible to record imaging data directly to RAM in the computer system, thus longer recording time can be achieved. We have recorded image sequences of fibrillating wave fronts for 20–30 s with a computer equipped with 128 Mbytes of RAM.

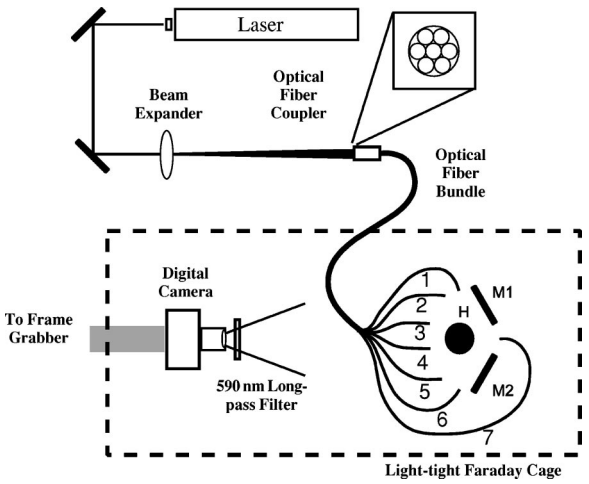


**Fig. 1** Experimental setup of the panoramic imaging system. The laser is delivered through a beam expander to the optical fiber coupler of a seven-fiber optical fiber bundle. Fibers 3 and 4 are directed toward the center of the heart. Fibers 2 and 5 deliver light to the mirrors, illuminating through reflection the side and back of the heart. Fibers 1 and 6 illuminate the posterior-lateral view of the heart. Fiber 7 either illuminates the back of the heart, or is used in conjunction with a laser power meter to monitor the light intensity. H: heart; M1, M2: mirrors.

Figure 1 shows the experimental setup of the panoramic imaging system. A 2-W solid-state frequency-doubled green laser (Millennia II, Spectra-Physics, Mountain View, CA) with a wavelength of 532 nm was used as the excitation light source. The laser beam was expanded and directed to the polished end of a fiberoptic bundle consisting of seven 1-mm plastic optical fibers (SP-SF-960, FIS Inc., Oriskany, NY). The exit end of each optical fiber serves as a stand-alone light source with an exit pupil of 29°. Laser output from the tips of optical fibers produced a speckle pattern, however the absorption and scattering of green laser in cardiac tissue reduced the uneven distribution of induced fluorescence. Consequently, the speckle in the acquired fluorescence images was less obvious. The flexibility of the optical fiber allows an easy positioning and aiming of these light guides around the heart. With this approach, a near uniform background illuminance around the heart can be obtained in less than 2 min of adjustment. Readjustment of illumination was seldom required during the experiment. The laser-induced fluorescence passes through a 590 nm long-pass orange filter (Schott Glass Technologies, Duryea, PA) before entering the camera.

Two mirrors positioned at the back of the heart were used to show the reflected images from the posterior views of the heart. These mirrors were mounted on a beam parallel to the imaging plane. The rotational angle of these mirrors was 15°–35° with respect to the image plane of the camera. The overlap between any two of the three views was approximately 10% of the surface area of the heart. The panoramic imaging system was developed to

image isolated rabbit hearts with physical dimensions of typically less than $40\times40\times50\,\mathrm{mm}^3$. With a typical field size of imaging at $96\times48\,\mathrm{mm}^2$ and a frame resolution of $128\times64$ pixels, each pixel corresponded to $0.75\times0.75\,\mathrm{mm}^2$ on the object plane.

### 2.2 HEART PREPARATION

New Zealand white rabbits weighing 4.4–5.5 kg were injected with 1000 units of heparin and 70 mg/kg sodium pentobarbital to induce deep general anesthesia. The heart was excised and the ascending aorta cannulated and secured for retrograde perfusion of the coronaries with a modified HEPES perfusate (108 mM NaCl, 5 mM KCl, 5 mM HEPES, 10 mM glucose, 20 mM C2H3O2Na, 1 mM MgCl2, 2.5 mM CaCl2). The perfusate was filtered through a micropore filter, adjusted to *p*H 7.35–7.45 with 1 N NaOH, oxygenated, and warmed to 37 $\pm0.5\,^{\circ}\mathrm{C}$. Coronary perfusion pressure was regulated to 80–95 mm Hg. The voltage-sensitive dye di-4-ANEPPS (Molecular Probes, Eugene, OR) was added to the perfusate at a concentration of 0.5 $\mu$M. The mechanical uncoupler diacetylmonoxime (DAM, Sigma) at 15 mM or D600 (Sigma) at 0.5 mg/l was added to the perfusate to minimize muscle contraction. To prevent heart motion due to perfusate dripping from the apex of the heart, a wick was sutured to the apex to allow smooth flow of perfusate. The wick partially blocked the view of the apex. However, selection of the size of the wick and a careful suturing can minimize such a block to less than $2\times2\,\mathrm{mm}^2$.

For monitoring purposes, electrocardiograms obtained from endocardial leads in the right ventricle were recorded during imaging. The use of internal leads avoided the obstruction of the panoramic view. The experiment was performed in a light-tight aluminum Faraday cage with a volume of approximately 1 $\mathrm{m}^3$ to prevent spurious ambient light from the room or computer screens from entering the imaging optics and increasing the noise level of the images.

### 2.3 IMAGE PROCESSING

In principle, an estimate of the distribution of the transmembrane potential ($S_n$) is obtained from a recorded epifluorescence image, $F_n$, with

$$S_n=-(F_n-F_{\mathrm{rest}})/F_{\mathrm{rest}}, \tag{1}$$

in which $F_{\mathrm{rest}}$ is the fluorescence intensity obtained from the resting tissue. The minus sign represents a decrease in fluorescence intensity with a more positive $V_m$.

With CCD video imaging, the $V_m$ information has been extracted using two approaches based on subtraction and division.[1,8] The subtraction approach is based on assumptions of a near-uniform $F_{\mathrm{rest}}$ distribution in the imaging field and a constant modulation of $F_{\mathrm{rest}}$ by $V_m$. Thus Eq. (1) can be simplified to

$$S_n=-(F_n-F_{\mathrm{rest}}) \tag{2}$$

using the intensity variation as the signal. The division operation has the implied advantage of correction for intensity nonuniformity and fluctuation in $F_{\mathrm{rest}}$. It is also preferable if quantitative measures of the $V_m$ distribution are desired. A background fluorescence intensity of the imaging field should be estimated before the division operation. This is straightforward for imaging stimulated activation in a small area of the tissue, in which the tissue status is known before the stimulation. For panoramic imaging of the whole heart, especially during irregular propagation such as fibrillation, the knowledge of $V_m$ at any time cannot be obtained. A good estimate for $F_{\mathrm{rest}}$ is the maximum value of every pixel in a sequence of images encompassing several cardiac cycles, assuming that the pixel intensity would return to the $F_{\mathrm{rest}}$ value at a certain time during the recording interval.

The raw image data may be visualized after simple operations such as background subtraction or division. However, in order to obtain quantitative measures of wave front dynamics such as activation isochrones, action potential duration, and conduction velocity, the noise level has to be reduced. Traditionally, this process was performed only in the spatial domain,[1,5] and some recent efforts have started to characterize the amount of signal-to-noise improvement with different filtering techniques.[9] The noise-reduction algorithms could take advantage of the high spatial and temporal resolutions, providing simultaneous operations across both the spatial and temporal domains. In this study, we used a simple $3\times3\times3$ moving average noise-reduction algorithm. The pixel intensity was replaced by the average of 27 neighboring pixels in the spatio-temporal domain. Such a type of linear filtering reduced the sharpness of the wave front by smoothing out the high frequency components in the signal. Therefore, an activation upstroke is smeared across three frames and nine neighboring pixels.

## 3 RESULTS

### 3.1 INTENSITY DISTRIBUTION

The factors determining the fluorescence intensity recorded from the heart include illumination, staining, and tissue condition. Figure 2(A) shows an example of a raw fluorescence recording from a diastolic heart, with Figure 2(B) showing contour plots for the intensity distribution. The center image is the frontal view of the heart, predominantly the anterior left ventricle. Under such an orientation, the right image shows mostly the reflection of the posterior left ventricle, and the left image shows

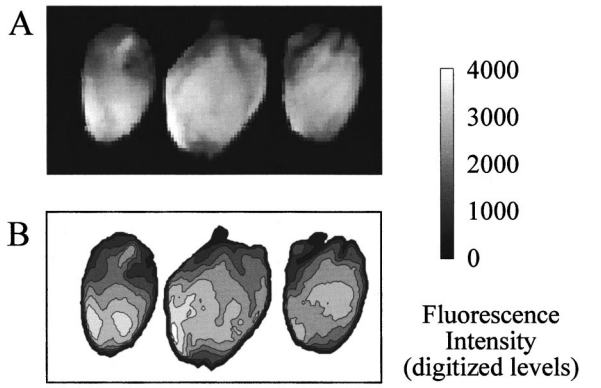


**Fig. 2** Distribution of fluorescence intensity from a resting heart. (A) the raw recording, (B) iso-intensity contour of the image in (A). Notice the steep intensity gradient along the edges of all three views. Frame size: $100 \times 50$ mm$^2$. The side views are not inverted, and the anatomical landmarks are similar to Figure 3(A).

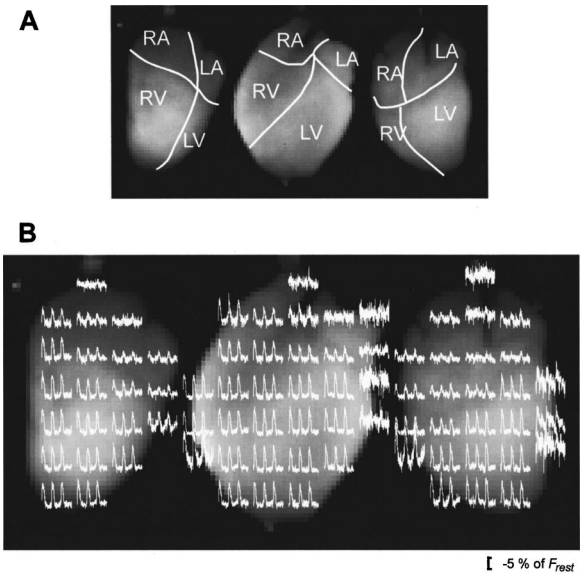


**Fig. 3** (A) Anatomical landmarks of the heart. (B) Frame-to-frame variation of fluorescence intensity in selected pixels due to a pulse stimulation from a bipolar electrode inside the right ventricle.

mostly the reflection of the right ventricle. The intensity contours show a steep gradient along the edges of all three views, as seen by closely spaced iso-intensity contour lines. The high intensity gradient prohibits determination of electrical signal data from the edge of each image, but overlap of the three views compensates for this situation, because signal can be obtained from at least one of the three views. In a typical setup, the angular overlap between any two views of the heart was restricted to $30° \pm 15°$.

For a 12 bit digital camera, saturation of camera exposure would obtain a digitized count of 4095. To maintain proper signal-to-noise level, we used a criterion that pixel intensity in the recorded area on resting tissue had to be more than 50% of the saturation level. A fully depolarized action potential corresponds to 5%–10% of the background intensity, which needs to be high enough to take advantage of the dynamic range in the system. Low fluorescence intensity reduces the digitized resolution and the signal-to-noise level of the optical transmembrane potential. This criterion is fulfilled in Figure 2, because the intensity from the entire ventricular area is greater than 2000 digitized counts. In most cases, due to destruction of the atrial tissue for endocardial electrode insertion, the intensity from the atria is not sufficient for meaningful study. However, the recording condition can be improved significantly by maintaining the intactness of the atria.

### 3.2 DISTRIBUTION OF APA AMPLITUDE

The relative change of the fluorescence intensity with respect to that of the resting tissue corresponds to the change in transmembrane potential. Figure 3 shows traces of pixel intensity variation overlapping an original image from a sequence of 300 frames, corresponding to a recording time of slightly less than 1 s, with the heart under periodic pacing at 3 Hz. These traces are centered at the corresponding pixel locations, and were inverted to account for a negative relationship as described in Eq. (1), and to show the more familiar look of transmembrane potentials. In this example, the variation from $F_{\text{rest}}$ level during the maximum action potential amplitude is approximately 7%–8% of $F_{\text{rest}}$ in the left ventricle, 6%–7% in the right ventricle, and only 3%–4% in the atria.

The distribution of signal amplitude in three hearts is shown in Figure 4. The upper regions of

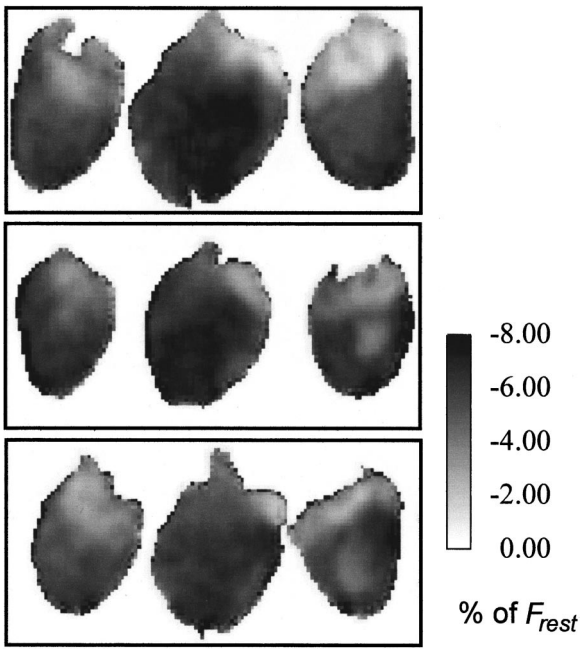


**Fig. 4** Distribution of maximum signal amplitude over the entire cardiac cycle in three hearts.

these images are the atrial tissue and have the lowest amplitude. This is due to imperfect perfusion of the atria. In contrast, signal amplitude obtained from the ventricles is mostly larger than a 5% modulation of the background fluorescence. Signal amplitude in the posterior left ventricle is the lowest.

### 3.3 PANORAMIC VIEW OF WAVEFRONT

Figure 5 shows three original traces and the corresponding traces after a $3\times3\times3$ moving average of adjacent pixels centered on the pixel under consideration. Clear visualization of wave front propagation became possible after the spatio-temporal smoothing. Figure 6 shows two different representations of an activation sequence due to stimulation from a pacing pulse. The number of frames was reduced to half of the original sequence. Therefore, the frame interval is 6.2 ms in Figure 6. A 20 frame sequence of percentage variation in background fluorescence intensity [$S_n$ in Eq. (1)] is shown in Figure 6(A). The difference of successive frames ($S_n - S_{n-1}$) representing the propagation of activation wave fronts is illustrated in Figure 6(B). In these images, the side views were flipped left to right to have a contiguous anatomy in the images. The activation started from the lateral right ventricle, propagated through both the anterior and posterior left ventricle, and finally met in the lateral left ventricle. Apparent tissue repolarization started from the lateral right ventricle [frame 11 in Figure 6(A)], as the pseudocolor changed from yellow to red. In frame 16, the only remaining region of yellow corresponded to the base on the left ventricle, representing a long action potential duration (APD) in this region.

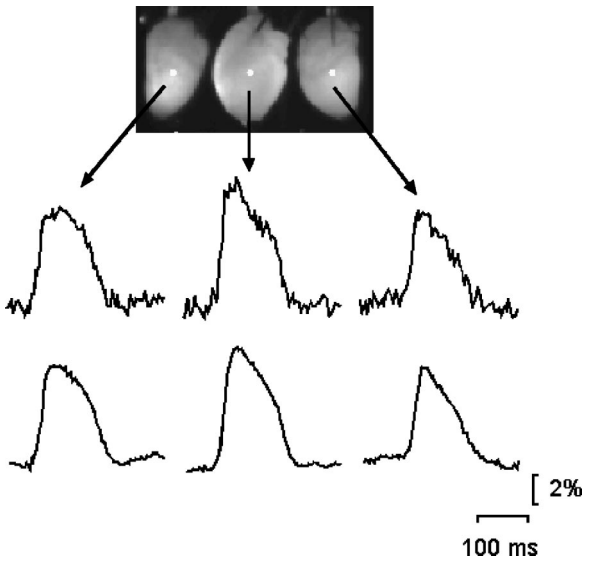


**Fig. 5** Results of smoothing with $3\times3\times3$ spatio-temporal averaging. The top row shows fluorescence intensity variation from a selected pixel in each of the three views. The smoothed traces are shown in the lower row directly below their original traces.

Figure 7(A) shows an isochronal map constructed from the same data set as shown in Figure 6 based on a 50% crossover of maximum $S_n$ in those frames. An isochronal map represents a compact illustration of the activation and repolarization sequence. It should be noted that the isochronal map shows a slightly different activation sequence from the difference images. This is because the definition of isochrones implies a normalization of signal amplitude, whereas the difference image does not normalize for different signal amplitude at different locations on the heart surface. The difference image offers a fast means of visualizing wave front propagation. However, isochrones constructed with normalized optical potential should be used for quantitative analysis.

An important advantage of optical recording is the capability to measure the repolarization as well as activation. An isochronal map of repolarization is shown in Figure 7(B). Because the relative lower signal-to-noise ratio of the CCD camera prohibits the use of the derivative method to detect repolarization, as was proposed for the data from photodiode recordings,[4] the repolarization map was determined with a 90% repolarization from the peak depolarization in each pixel. From Figure 7, the repolarization process did not follow the time sequence of activation, therefore showing a dispersion of APD around the heart. The base of the left ventricle (area encircled by the frame index 62) appeared to have the longest APD.

The panoramic imaging technique expands the view to cover the entire heart surface, thus allowing measurement of global phenomena such as fibrillating wave fronts and tissue response to defibrillatory shocks. Figure 8 shows isochronal maps of activation from a fibrillating heart in two different cycles. The signal amplitude during fibrillation as measured by the variation of fluorescence intensity from the resting tissue was lower than with paced rhythm. The activation was determined by a 50% crossover between the minimum and maximum signal amplitude over the entire episode of recording, and the propagation pathways were indicated with arrows overlapping the isochronal maps. In the cycle illustrated with Figure 8(A), the activation started from the lateral RV, bifurcated in the frontal (center view) and posterior (left view) LV, and one of the branches propagated downward and reentered through the apex of the RV. In Figure 8(B), a conduction block in the posterior RV (right view) caused reentry through the apex of the RV, but the direction of wave rotation was counterclockwise (left view) and was opposite to the direction in Figure 8(A).

## 4 DISCUSSION

The panoramic imaging technique provides simultaneous, dynamic information on wave front activation and propagation over the entire heart surface.

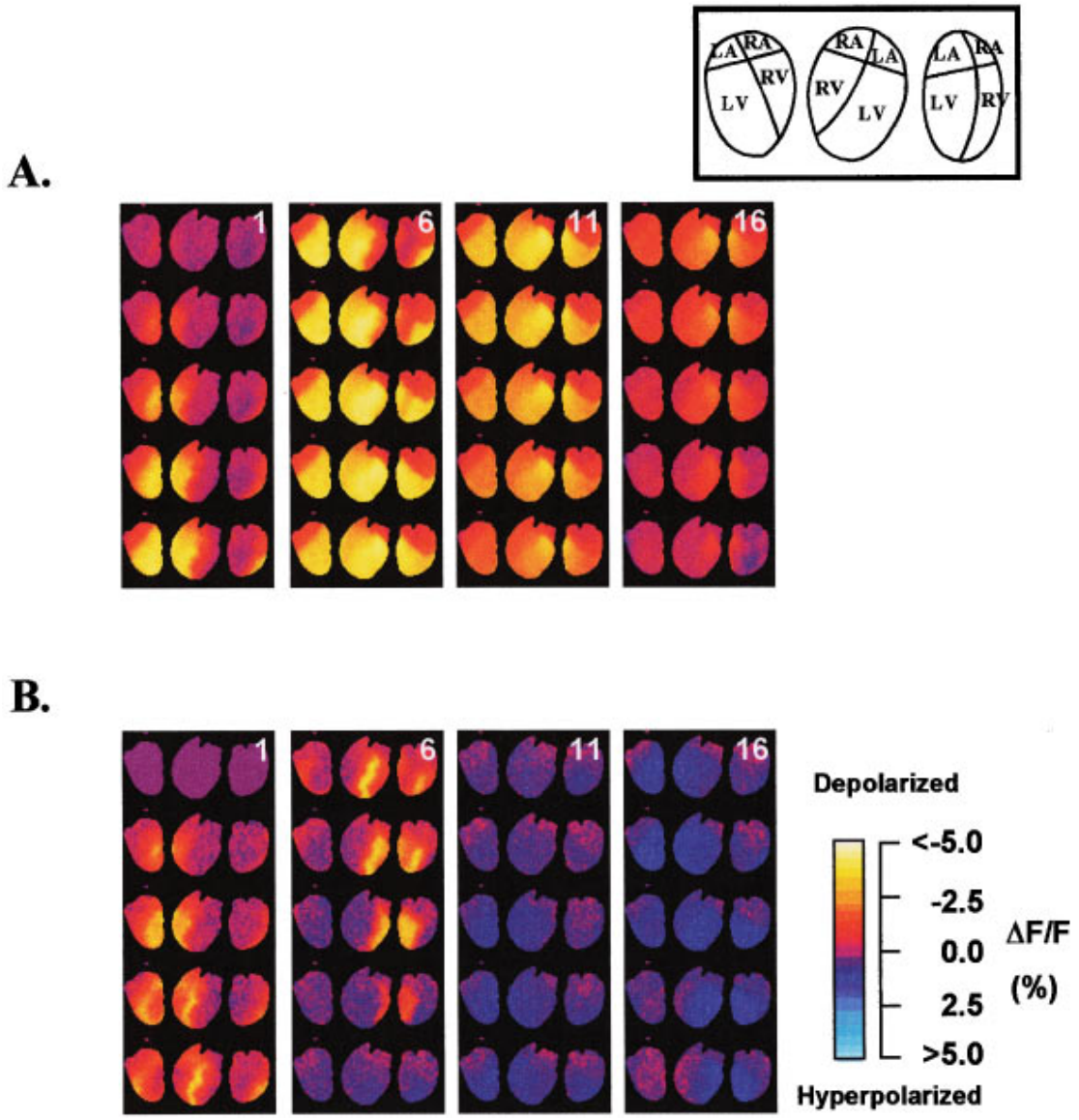


**Fig. 6** Two pseudo-color representations of wave front dynamics from a paced rhythm. (A) Percentage of intensity variation from the resting state. (B) Differences of fluorescence intensity from successive images. The approximate anatomy of the heart is shown in the inset (LA: left atrium, LV: left ventricle, RA: right atrium, RV: right ventricle). The numbers on the isochrones show the frame index starting from the stimulus. These images were coded by pseudocolors of purple, red, and yellow, indicating low–high amplitude. The number of frames was reduced by skipping every other frame in the raw data, resulting in a frame interval of 6.2 ms.

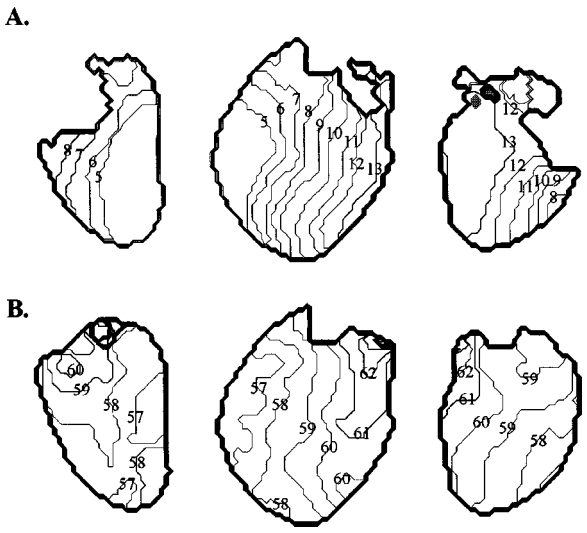


**Fig. 7** Representation of isochronal maps for (A) activation sequence and (B) repolarization pattern. Frame interval: 3.1 ms.

The feasibility of our panoramic surface imaging derives from the fact that there is little concavity on the surface of heart geometry, especially in the ventricular areas. Hence a full 3D view can be revealed with mirror images. The successful development of this technique removed a significant constraint in cardiac optical mapping, which was previously performed only on a single view of the heart, without the need for multiple cameras. However, we emphasize that the current technique is limited to recording only the epicardium; further development is required to obtain information on transmural and endocardial activation and propagation.

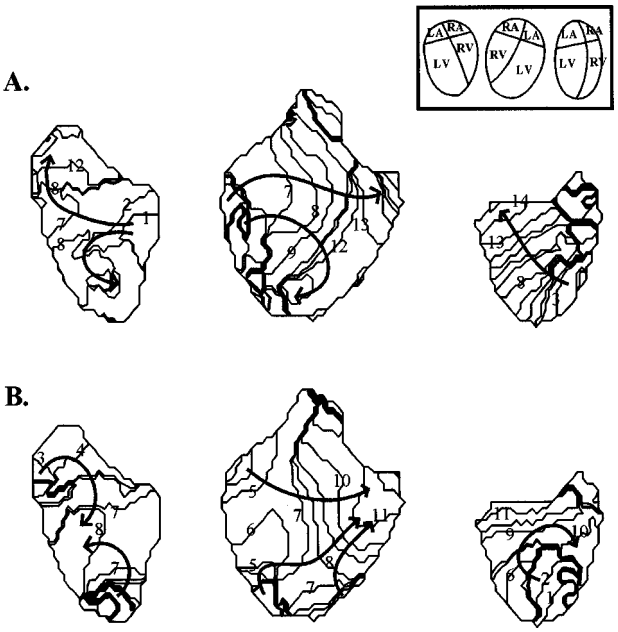


**Fig. 8** Isochronal map of tissue activation during fibrillation in two different cycles. The numbers indicate the frame number relative to the start of the cycle. The numbers on the isochrones show the frame index starting from the onset of the cycle. Frame interval: 3.1 ms.

The system described in this paper was developed around an isolated rabbit heart model, with the emphasis on measuring ventricular electrical activities. However, because the atria were cut open for insertion of endocardial electrodes, the atrial tissue is not well perfused, and little activity can be measured from the atria. Future development of the panoramic imaging technique should aim at maintaining the atrial functions for studies of electric propagation around the entire epicardium. Another obvious deficiency of the current system is an inefficient use of the full CCD. The format of the panoramic images resulted in a dead space of around 30%–40% depending on the size of the heart, so that there are approximately 5000–6000 active pixels in each image. The pixels outside the tissue contain no information to be extracted, and should be compressed to reduce storage and processing requirements.

The panoramic imaging technique described in this paper requires the application of mechanical uncoupling agents such as DAM or D600 to inhibit muscle contraction. This prohibits quantitative studies of cardiac electrophysiology when the effects of uncoupling agents may be augmented or complicated by other external agents such as antiarrhythmic drugs or electrical shocks.[10] When imaging only one view of a contracting heart, the movement may be limited by gently pushing the heart against a glass plate.[7] This method cannot be used for obtaining a panoramic view, because any external mechanical constraining device would block the view of at least some part of the heart surface. It is still possible to obtain qualitative data based on sequential subtraction algorithms. The fast frame rate is especially favorable for optical imaging the heart without uncoupling agents. This is because at high frame rates, the heart may be considered as stationary during a short interval, allowing reliable extraction of the activation pattern or propagation wave front. Cardiac cells are normally activated in less than a millisecond, therefore we estimate that a camera frame rate of 1000 frames/s is the minimum required speed to image preparation without uncoupling agents. However, the information of repolarization cannot be reliably obtained under the assumption of temporary stationariness.

At present, we are visualizing the wave fronts using the raw image format, such as the 2D view in Figure 6. In addition, the side images are flipped left to right to offer a contiguous view of the anatomical features. By acquiring the geometry of the heart, it should be possible to perform 3D visualization and measurement. This is important in that the heart curvature should be considered in calculating the distribution of conduction velocity. We are currently developing the measurement and analysis techniques that are required to combine the three

planar images into a three dimensional computer model of the cardiac surface.

### Acknowledgments

This study was supported in part by NIH Grant Nos. P01HL46681, R01HL58241, and T32HL07411, and a Biomedical Engineering Research Grant from the Whitaker Foundation.

## REFERENCES

1. J. M. Davidenko, A. M. Pertsov, R. Salomonsz, W. T. Baxter, and J. Jalife, ''Stationary and drifting spiral waves of excitation in isolated cardiac muscle,'' *Nature (London)* **355**, 349–351 (1991).
2. D. M. Dillon, ''Synchronized repolarization after defibrillation shocks. A possible component of the defibrillation process demonstrated by optical recording in rabbit heart,'' *Circulation* **85**, 1865–1878 (1992).
3. S. B. Knisley, T. F. Blitchington, B. C. Hill, A. O. Grant, W. M. Smith, T. C. Pilkington, and R. E. Ideker, ''Optical measurements of transmembrane potential changes during electric stimulation of ventricular cells,'' *Circ. Res.* **72**, 255–270 (1993).
4. I. R. Efimov, D. T. Huang, J. M. Rendt, and G. Salama, ''Optical mapping of repolarization and refractoriness from intact hearts,'' *Circulation* **90**, 1469–1479 (1994).
5. J. P. Wikswo, Jr., S.-F. Lin, and R. A. Abbas, ''Virtual electrodes in cardiac tissue: A common mechanism for anodal and cathodal stimulation,'' *Biophys. J.* **69**, 2195–2210 (1995).
6. D. S. Rosenbaum, D. T. Kaplan, A. Kanai, L. Jackson, H. Garan, R. J. Cohen, and G. Salama, ''Repolarization inhomogeneities in ventricular myocardium change dynamically with abrupt cycle length shortening,'' *Circulation* **84**, 1333–1345 (1991).
7. A. Kanai and G. Salama, ''Optical mapping reveals that repolarization spreads anisotropically and is guided by fiber orientation in guinea pig hearts,'' *Circ. Res.* **77**, 784–802 (1995).
8. S.-F. Lin, R. A. Abbas, and J. P. Wikswo, Jr., ''High-resolution high-speed synchronous epifluorescence imaging of cardiac activation,'' *Rev. Sci. Instrum.* **68**, 213–217 (1997).
9. I. Banville, R. A. Gray, and R. E. Ideker, ''Optimization of high-resolution video imaging system to study cardiac spatiotemporal patterns,'' *Ann. Biomed. Eng. (Suppl.)* **26**, S-19 (1998).
10. Y. Liu, C. Cabo, R. Salomonsz, M. Delmar, J. Davidenko, and J. Jalife, ''Effects of diacetyl monoxime on the electrical properties of sheep and guinea pig ventricular muscle,'' *Cardiovasc. Res.* **27**, 1991–1997 (1993).